Supporting Information for

Effect of the electric field on the agyrotropic electron distributions

C. -H. Gao [1,2], B. -B. Tang [1], W. Y. Li [1], C. Wang [1,2], Yu. V. Khotyaintsev [3], D. B. Graham [3], D. J. Gershman [4], A. C. Rager [6,5], B. L. Giles [5], P. -A. Lindqvist [7], R. E. Ergun [8], C. T. Russell [9], and J. L. Burch [10]

[1]State Key Laboratory of Space Weather, National Space Science Center, Chinese Academy of Sciences, Beijing, China.
[2]College of Earth and Planetary Sciences, University of Chinese Academy of Sciences, Beijing, China.
[3]Swedish Institute of Space Physics, Uppsala, Sweden.
[4]Department of Astronomy, University of Maryland, College Park, MD, USA.
[5]NASA Goddard Space Flight Center, Greenbelt, Maryland, USA.
[6]Department of Physics, Catholic University of America, Washington, DC, USA.
[7]KTH Royal Institute of Technology, Stockholm, Sweden.
[8]Laboratory of Atmospheric and Space Physics, University of Colorado Boulder, Boulder, Colorado, USA.
[9]Department of Earth and Space Sciences, University of California, Los Angeles, California, USA.
[10]Southwest Research Institute, San Antonio, Texas, USA.

1 Contents of this file

1. Figure S1 - S4
2. Supplementary Text

2 Description of the test particle method

The test particle method is applied to generate the electron distributions in the plane perpendicular to the local magnetic field based on the Liouville mapping of the electron phase space density ($df/dt = 0$). When the initial conditions are set, the electron phase space density at a specified location are estimated along the electron gyro-orbit. An example is provided in Fig. S1, and the link for the Matlab code used in the present study can be found in the acknowledgment. Meanwhile, it is noting that the agyrotropic elec-

Corresponding author: B. -B. Tang and W. Y. Li, bbtang@spaceweather.ac.cn, wyli@spaceweather.ac.cn

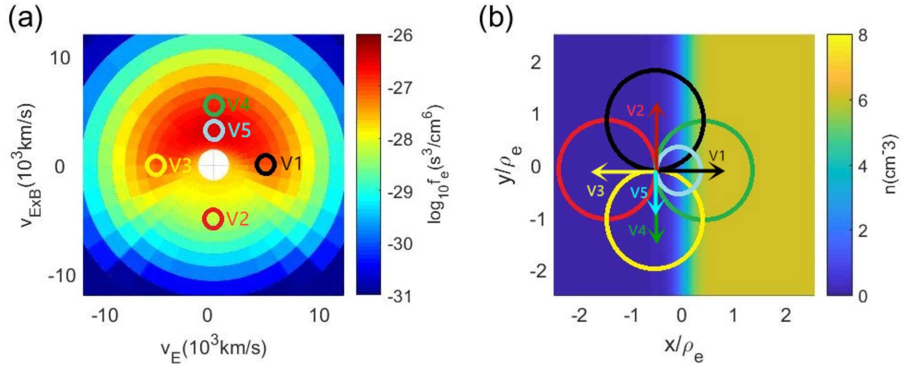

Figure S1. Construction of the electron distributions in the test particle simulations. The electron phase space density (a) at a specified location are estimated from the averaging the phase space density along the electron gyro-orbit (b).

tron distributions generated by the test particle method not is self-consistent, but the similarity between the observations and the test particle results shown in the main text suggests the test particle method can reasonably capture the key process of the generation of the agyrotropic electron distributions. Therefore the test particle method is basically applicable here, but more self-consistent simulations, such as the particle in-cell simulation, are needed if we want to get more accurate results.

3 Test particle results from the different settings of the electric field

In the main text, we have shown a strong local electric field can effectively accelerate electrons to form agyrotropic electron distributions, but the favorable parameters for this electric field has not been fully addressed. Here we present four different settings of the electric field referred to this problem, which are

(a) |B| = 30 nT, n = 6 cm^{-3}, T_e = 60 eV, and E(x) = g(x) (Fig. S1a1).

(b) |B| = 30 nT, n = 6 cm^{-3}, T_e = 60 eV, and E(x) = g(x) (Fig. S1b1).

(c) |B| = 30 nT, n = 6 cm^{-3}, T_e = 60 eV, and E(x) = g(x) (Fig. S1c1).

(d) |B| = 10 nT, n = 6 cm^{-3}, T_e = 60 eV, and E(x) = g(x) (Fig. S1d1).

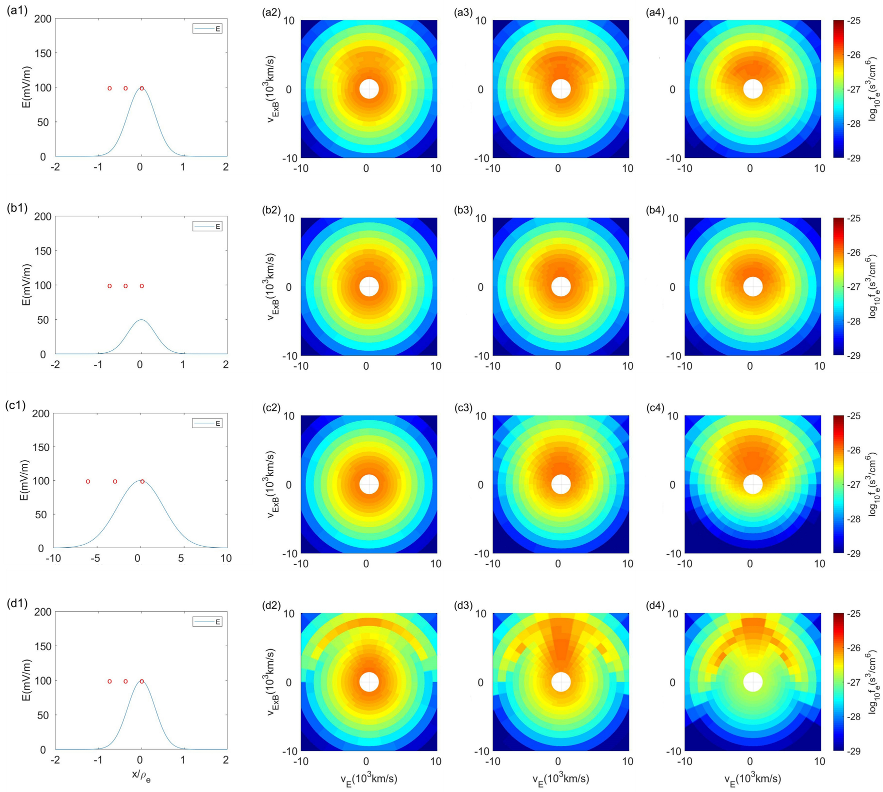

Figure S2. Test particle results under different settings for the electric field. (a1) The setting of the electric field. Three red circles indicate the location where electron distributions generated in (a2 - a4). (b1 - b4), (c1 - c4), and (d1 - d4) are similar to (a1 - a4), but for the different settings of the electric field.

where g(x) = $E_0 \exp(-x^2/\sigma^2)$. The peak electric field E_0 of g(x) in case a, b, c and d are 100 mV/m, 50 mV/m, 100 mV/m, and 100 mV/m, and the corresponding σ are $0.3\rho_{e,a}$, $0.3\rho_{e,a}$, $2.5\rho_{e,a}$ and $0.3\rho_{e,d}$, where $\rho_{e,a}$, and $\rho_{e,d}$ are the electron thermal gyroradius in case a and d. The parameters set in case a is the same with the case 4 in the main text, where the potential drop is about (Φ) 60 V and the full width at half maximum (FWHM, h) is about 0.75 $\rho_{e,a}$, and agyrotropic electron distributions are generated (Fig. S2a2 - a4). If we decrease the electric field by 50% (Fig. S2b1), meaning the corresponding potential drop is much smaller than the electron temperature, electrons can not be effectively accelerated out of the electron core to form agyrotropic electron distribution (Fig. S2b2 - b4). If the width of the electric field is much larger than the the electron thermal gyroradius (Fig. S2c1), we can only find drifting maxwellian distributions (Fig. S2c4). Based on these test particle runs, we suggest that the favorable conditions of the strong local electric field to generated agyrotropic electron distributions are (1) its electrostatic potential should be comparable to or larger than the electron temperature, and (2) its width should not be larger than the electron thermal gyroradius. As the electron thermal gyroradius is also a function of the background magnetic field, we suggest that agyrotropic electron distributions are more favorable to be generated with weaker magnetic field (Fig. S2d2 - d4), which allows a larger potential drop to accelerate electrons.

4 Reproducing the “finger” structure with a time-dependent electric field

In the main text, we have successfully reproduced the measured electron “finger” structure by assuming a virtual detector that moves towards a static electric field (Fig. S4a1), but the “observed” electric field by the virtual detector during the related time interval is different with MMS observations (Fig. S4a2). How can we eliminate this difference? One possible solution is to introduce some temporal variations to this strong electric field, and the parameters of this electric field should be reconsidered due to this time-varying effect. The potential drop can be estimated by comparing the decomposed 7.5 ms electron distributions, as the first 7.5 ms electron distribution is roughly gyrotropic (Fig. 4a2). The curve of the phase space density of the agyrotropic distributions (the solid black line in Fig. S4b) is shifted to maximize the coefficient of determination (R^2) with the curve of the gyrotropic distributions (the green line in Fig. S3b), and the shifted energy of the best fit is taken as the acceleration potential, which is approximately 100 eV. The peak magnitude of the electric field (E_0) is a free parameter, which is set to 150 mV/m here,

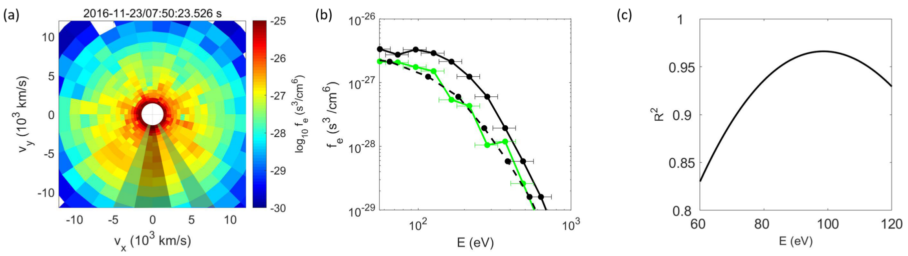

Figure S3. The observed electron "finger" structure. (a) the measured 30 ms electron "finger" structure in DBCS coordinates. (b) The electron phase space density measured along the negative y direction at the first 7.5 ms (green) and the rest time interval (black). The dotted black line is the shifted solid black line by $\sim$ 100 eV. (c) The coefficient of determination (R^2) between the green line and the shifted black line with different shift energies.

so that it is convenient for the virtual detector to "observe" an electric field of $\sim$ 100 mV/m. The electric field function then can be functioned as $E_0 \exp(-x^2/\sigma^2)h(t)$, where $h(t)$ is a sine-type function to include the temporal variations (Fig. S4b1 and b2).

Similar to the electron acceleration due to a static electric field, a time-dependent electric field can also successfully accelerate electron to form agyrotropic electron distributions (Fig. S4b3 - b5), as it satisfies the conditions of a strong local electric field. By introducing the time-varying effect, the relative speed of the virtual detector can decrease to $\sim$ 9 km/s, which is more consistent with the timing result from the observations on 23 November 2016. The "recorded" electric field from the virtual detector matches better with observations as well (Fig. S4b2). Though the peak amplitude of this electric field is artificially set in test particle runs, we infer that this large-amplitude short-lived localized electric field might be a more physical picture responsible for the generation measured electron "finger" structures, as it meets the expectations of highly fluctuating plasma environments in observations.

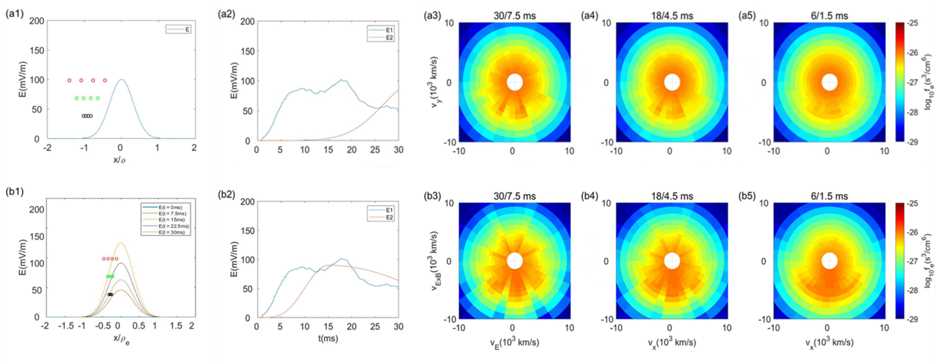

Figure S4. The reproducing of the electron “Finger” structure with a static electric field and a time-varying electric field. (a1) The initial setting of the static electric field. The red/green/black circles indicate the central positions for the four intermediate electron distributions at a sampling rate of 30/18/6 ms. (a2) The electric field ”observed” by a virtual detector at a sampling rate of 30 ms (red) and MMS observations of the electric field (blue). (a3 - a5) The composite of electron distributions at a sample rate of 30 ms, 18 ms and 6 ms. (b1 - b5) Similar to (a1 - a5), but the electric field is time-dependent.